A Kinetic Model for the Oxidation of Toluene near 1200 K

J. L. Emdee, K. Brezinsky,* and I. Glassman

Mechanical and Aerospace Engineering Department, Princeton University, Princeton, New Jersey 08544-5263
(Received: May 20, 1991; In Final Form: November 18, 1991)

An improved kinetic model for the high-temperature oxidation of toluene has been developed using previously established reaction mechanisms for benzene and toluene. The model is compared to benzene and toluene flow reactor experiments near 1100 and 1200 K, respectively. Fuel decay rates and many intermediate species profiles are reproduced successfully for both lean and rich equivalence ratios. A linear sensitivity analysis indicated that the reaction mechanism was most sensitive to the rate constant of $C_6H_5CH_3 + O_2 \rightarrow C_6H_5CH_2 + HO_2$ (71). A value of $k_{71} = 3.0 \times 10^{14} \exp(-20700/T)$ cm^3/mol/s was found to fit the experimental data best. The model revealed that the presence of resonantly stable radicals such as benzyl and phenoxy can inhibit the reaction rate of the fuel by removing H atoms from the system. Specific shortcomings of the model are also discussed.

I. Introduction and Background

The use of aromatic hydrocarbons in today's gasolines and jet fuels is a trend that is expected to continue in the future. Aromatics offer many advantages such as a high energy density[1] and a high knock rating.[2] In working toward a comprehensive understanding of aromatic combustion, the high-temperature oxidation mechanism of toluene has been studied extensively in this laboratory.[3-8] The mechanistic details gained in those studies have indicated that at temperatures near 1000 K and 1 atm pressure the early time oxidation characteristics are dominated by side-chain chemistry followed by aromatic ring attack. The reactions of the small molecule fragments of the aromatic ring, for the most part, occur later in the reaction sequence. Therefore, a modest sized model for the oxidation of toluene near 1200 K was developed and is presented here. This model captures the early time chemistry and the essential details of the later time small molecule reactions.

To the authors' knowledge, there are only two previous attempts at modeling the oxidation of toluene.[9,10] McLain et al.[9] modeled CO/CO_2 concentrations and induction times for the oxidation of both benzene and toluene at 1700-2800 K. Using global steps for the reaction of phenyl and benzyl with oxygen molecule, McLain et al.[9] were able to match well the experimental induction times.

The model of Bittker[10] was based on the oxidation chemistry outlined by Brezinsky[6] but used a benzene submodel[11] which was unsatisfactory in reproducing the fuel decay in benzene flow reactor experiments. (During the preparation of this manuscript the authors became aware of an updated benzene model by Bittker;[12] however, this model has not been incorporated into Bittker's toluene model.[10]) Ignition delay times and flow reactor data were compared to the toluene model predictions with fair agreement. Due to the importance of an accurate submechanism for benzene, the toluene model of Bittker[10] is questionable. Bittker's[10] model does suggest some of the important points of the mechanism, however. A sensitivity analysis showed that the toluene decay was most sensitive to the reaction of toluene with molecular oxygen:

$$C_6H_5CH_3 + O_2 \rightarrow C_6H_5CH_2 + HO_2$$

As will be discussed later, this reaction was also found to be important in this work.

With the mechanistic and rate constant information gained over the past few years, a model for the oxidation of toluene was constructed which does not rely heavily on global steps. This model is capable of reproducing benzene oxidation experiments reasonably well and is not so large that it cannot be incorporated into combustion applications models such as those used to calculate laminar flame speeds. The model that has been developed is based largely on the mechanisms in Figures 1 and 2 given by Brezinsky.[6] The only major change to the Brezinsky[6] mechanism is the addition of the reaction $C_6H_5CH_3 + O_2 \rightarrow C_6H_5CH_2 + HO_2$ mentioned above.

II. Experimental Data for Model Verification

The data of Brezinsky et al.,[5] and Lovell et al.,[13] were used to verify the toluene model (see Table I). These data were from Princeton flow reactor experiments and include lean and rich equivalence ratios (Φ) with initial temperatures from 1100 to 1190 K. The experimental details are described in the individual papers.

Slight adjustments were made to the data presented in the above two references to reflect recent calibration of the flow reactor rotameters[14] and velocity profile.[15] The effect of these recent changes is to give reaction times which are approximately 15-20% shorter than given in the original papers. It should be noted that the velocity profile in the reactor tube is still under investigation. Further details regarding the reduction of the experimental data can be found in the thesis of Emdee.[14]

III. Description and Analysis of the Model

The thermodynamic properties of many of the chemical species used in the model are indicated in Table II. Species which are

(1) Goodger, E.; Vere, R. *Aviation Fuels Technology*; MacMillan Publishers Ltd.: London, 1985.
(2) ASTM Special Technical Publication No. 225; American Society of Testing Materials, Philadelphia, 1958.
(3) Euchner, J. A. A Study of the Oxidation of Toluene in a Flow Reactor. M.S.E. Thesis, Department of Mechanical and Aerospace Engineering, Princeton University, Princeton, NJ, 1980.
(4) Venkat, C.; Brezinsky, K.; Glassman, I. *Nineteenth Symposium (International) Combustion [Proceedings]*; The Combustion Institute: Pittsburgh, 1983; p 143.
(5) Brezinsky, K.; Litzinger, T. A.; Glassman, I. *Int. J. Chem. Kinet.* **1984**, *16*, 1053.
(6) Brezinsky, K. *Prog. Energy Combust. Sci.* **1986**, *12*, 1.
(7) Litzinger, T. A. The High Temperature Oxidation of Alkylated Aromatic Hydrocarbons. Ph.D. Thesis, Department of Mechanical and Aerospace Engineering, Princeton University, Princeton, NJ, 1986.
(8) Brezinsky, K.; Lovell, A. B.; Glassman, I. *Combust. Sci. Technol.* **1990**, *70*, 33.
(9) McLain, A. G.; Jachimowski, C. J.; Wilson, C. H. Chemical Kinetic Modeling of Benzene and Toluene Behind Shock Waves; NASA Tech. Paper 1472, 1979.
(10) Bittker, D. A. Detailed Mechanism of Toluene Oxidation and Comparison with Benzene; NASA Tech. Memo. 100261, 1988.
(11) Bittker, D. A. Detailed Mechanism of Benzene Oxidation; NASA Tech. Memo. 100202, 1987.
(12) Bittker, D. A. *Combust. Sci. Technol.* **1991**, *79*, 49.
(13) Lovell, A. B.; Brezinsky, K.; Glassman, I. *Twenty-Second Symposium (International) Combustion [Proceedings]*; The Combustion Institute: Pittsburgh, 1989; p 1063.
(14) Emdee, J. L. An Experimental and Modeling Study of the High Temperature Oxidation of the Xylenes. Ph.D. Thesis, Department of Mechanical and Aerospace Engineering, Princeton University, Princeton, NJ, 1991.
(15) Chang, E. Characterization of the Flow Field of the Flow Reactor; Undergraduate Independent Work, Mechanical and Aerospace Engineering Department, Princeton University, 1989.

0022-3654/92/2096-2151$03.00/0

TABLE I: Experimental Conditions for the Oxidation of Benzene and Toluene in a Flow Reactor at 1 atm[a]

		mole fraction × 10^6						
case no.	fuel	fuel	oxygen	nitrogen	ϕ	$T_{initial}$, K	T_{final}, K	ref
1	benzene	1406	16153	982441	0.65	1098	1117	13
2	benzene	1495	12301	986204	0.91	1096	1103	13
3	benzene	1457	7927	990616	1.38	1096	1098	13
4	toluene	1540	20015	987445	0.69	1188	1198	5
5	toluene	1616	10907	987477	1.33	1190	1190	5

[a] $\phi \equiv$ {[fuel]/[oxygen]}/{[fuel]/[oxygen] stoichiometric mixture}.

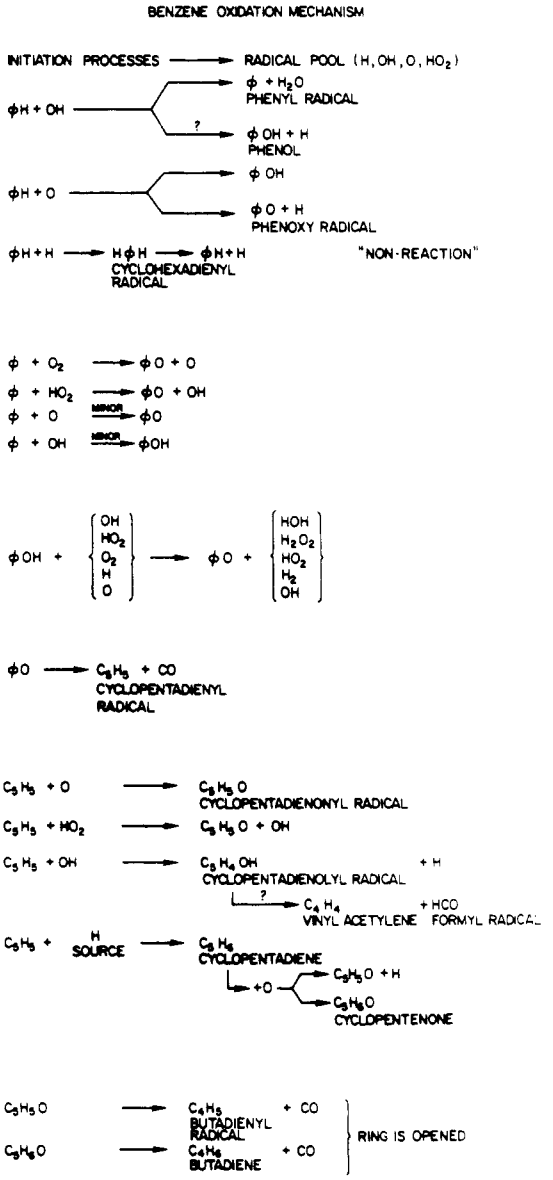

Figure 1. Benzene oxidation mechanism. Reprinted with permission from ref 6. Copyright 1986 Pergamon Press.

not indicated in Table II were taken from the work of Kee et al.[16] The thermodynamic properties of benzyl radical, $C_6H_5CH_2$, were taken from the recent comprehensive work of Hippler et al.[17] Their data support a larger heat of formation for benzyl than the widely used value recommended by Burcat[18] (ΔH_f = 47.8 kcal/mol). A higher value for the heat of formation is also supported by the recent work of Braun-Unkhoff et al.[19]

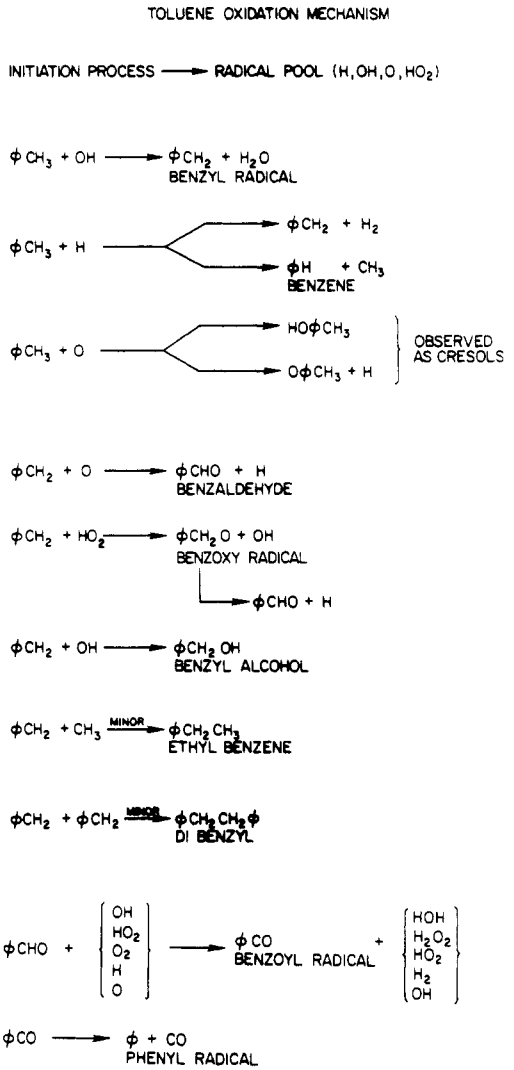

Figure 2. Toluene oxidation mechanism. Reprinted with permission from ref 6. Copyright 1986 Pergamon Press.

The model consists of 68 reactions forming a benzene submodel (Table III) and 62 additional reactions for the toluene model (Table IV). Since benzene is a key intermediate in the oxidation of toluene, the benzene submodel results will be considered before the toluene model is discussed.

A. Benzene Submodel. (i) Discussion of Reactions. The addition of O atom to benzene has been studied by many investigators with continued disagreement as to the products of reaction. Sibener et al.,[20] however, was able to show with molecular beam studies that the triplet biradical intermediate forms either phenol, C_6H_5OH, or phenoxy radical, C_6H_5O, and H atom. The work of Nicovich et al.[21] and Tappe et al.[22] support Sibener's[20] findings.

(16) Kee, R. J.; Rupley, F. M.; Miller, J. A. The Chemkin Thermodynamic Data Base; Sandia Nat. Lab. Report SAND87-8215, 1987.
(17) Hippler, H.; Troe, J. *J. Phys. Chem.* **1990**, *94*, 3803.
(18) Burcat, A. *Combustion Chemistry*; Gardiner Jr., W. C., Ed.; Springer-Verlag: New York, 1984; Appendix C.
(19) Braun-Unkhoff, M.; Frank, P.; Just, Th. A Shock Tube Study on the Decomposition of Benzyl Radical. Poster 197 presented at the *Symp. (Int.) Combust.*, *23* 1990.
(20) Sibener, S. J.; Buss, R. J.; Casavecchia, P.; Hirooka, T.; Lee, Y. T. *J. Chem. Phys.* **1980**, *72*, 4341.
(21) Nicovich, J. M.; Gump, C. A.; Ravishankara, A. R. *J. Phys. Chem.* **1982**, *86*, 1684.
(22) Tappe, M.; Schliephake, V.; Wagner, H. Gg. *Z. Phys. Chem.* **1989**, *162*, 129.

TABLE II: Thermodynamic Properties for Selected Species As Used in the Toluene Model[a]

species	ΔH_{f298}	S_{298}	$C_{p,300}$	$C_{p,400}$	$C_{p,500}$	$C_{p,600}$	$C_{p,800}$	$C_{p,1000}$	$C_{p,1500}$	ref
$C_6H_5CH_3$	11.95	76.46	40.98	44.80	48.34	51.61	57.43	62.36	71.37	18
$C_6H_5CH_2$	50.32	76.75	26.32	34.22	40.80	46.27	54.53	60.24	68.36	17
$C_6H_5CH_2OH$	-23.99	87.46	28.20	36.80	44.08	50.23	59.76	66.49	76.22	*b*
$C_6H_5C_2H_5$	7.15	86.21	30.71	40.83	49.34	56.47	67.43	75.11	86.25	48
bibenzyl	34.30	114.48	49.22	65.72	79.51	90.97	108.32	120.18	136.86	*b*
$HOC_6H_4CH_3$	-30.77	84.41	30.27	39.13	46.45	52.48	61.53	67.75	76.87	*c*
$OC_6H_4CH_3$	3.63	78.25	28.73	37.19	44.22	50.02	58.70	64.55	72.62	*b*, *c*
$C_6H_5C_2H_3$	35.44	82.41	29.02	38.29	45.95	52.26	61.71	68.18	77.63	48
C_6H_5CHO	-8.70	83.49	25.87	33.40	39.83	45.29	53.79	59.74	67.95	*b*
C_6H_5CO	26.10	84.90	25.73	32.71	38.61	43.57	51.17	56.39	63.44	*b*
C_6H_6	19.81	64.37	19.92	27.09	33.25	38.38	45.87	51.05	58.32	16
C_6H_5	78.50	68.91	19.00	25.45	30.97	35.53	42.10	46.59	52.77	49
C_6H_5OH	-23.03	75.33	24.94	32.39	38.63	43.68	50.73	55.57	62.37	49
C_6H_5O	11.40	73.57	22.71	29.77	35.74	40.61	47.50	52.17	58.53	49
C_5H_6	32.00	64.46	16.67	23.12	28.70	33.39	40.31	45.10	51.83	16
C_5H_5	54.31	62.41	17.34	23.89	29.16	33.39	39.46	43.39	48.86	27
C_5H_5O	43.35	71.38	21.13	27.41	32.65	36.99	43.54	48.00	54.09	*b*
C_5H_4O	4.15	67.13	18.33	24.10	28.95	33.01	39.16	43.36	48.96	*b*
C_5H_4OH	12.35	74.27	22.17	28.65	33.79	37.85	43.58	47.28	52.86	*b*
C_4H_6	26.34	66.62	22.36	25.95	29.17	32.04	36.82	40.51	46.32	26
C_4H_5	80.21	69.81	19.71	23.82	27.18	29.93	34.08	37.02	41.80	50
C_4H_4	73.62	66.64	17.59	21.16	24.20	26.71	30.41	33.18	37.33	16
C_2H_4	12.54	52.38	10.23	12.79	14.94	16.83	20.05	22.51	26.22	16
C_2H_3	66.61	57.01	10.83	12.42	13.84	15.12	17.28	19.02	21.87	50
C_2H_2	54.20	48.02	10.62	11.99	13.08	13.95	15.27	16.31	18.28	16
HO_2	3.00	54.73	8.34	8.95	9.49	9.97	10.78	11.39	12.45	36

[a] Properties for species not listed were taken from the compilation of Kee et al.[16] Units: kcal/mol for ΔH_f and cal/mol/K for S and C_p. [b] Estimated using group additivity methods.[32,51] [c] Based on the average of *o*-, *m*-, *p*-cresol properties.[52]

The branching ratio for phenoxy or phenol formation has not been determined conclusively. Cvetanovic,[23] in reviewing O atom reaction rate constant parameters at 298–867 K, has suggested that only 13% of the adduct rearranges to phenol. Mulder and Louw[24] used product analysis of chlorobenzene oxidation experiments at 520–1080 K to determine that O atom reaction with benzene forms mainly phenol. Recent work by Lovell et al.[13] suggests that the phenol formed during flow reactor benzene experiments was a result of O atom addition. That conclusion was based on the results of the perturbation of the radical pool by the addition of NO_2 to the gas stream.

Recently, QRRK calculations[25] were performed by the authors in order to better evaluate the branching ratio. The formation of phenoxy radical was modeled as the simple loss of a hydrogen from the excited benzene plus oxygen atom adduct. The high-pressure activation energy barrier necessary for the QRRK calculation[26] was assigned a value of 6.9 kcal/mol which includes an intrinsic activation energy of about 4 kcal and a small endothermic barrier. The preexponential A value of 2.7×10^{13} s^{-1} was calculated from the change in entropy of the reaction and the reverse A factor which was set equal to that for hydrogen addition to an aromatic ring.[27] The formation of phenol was modeled as an isomerization of the adduct via a three-member transition state with a ring strain of 27 kcal/mol and an intrinsic activation energy of about 4 kcal/mol. The preexponential value was set at 3.3×10^{12} based on thermodynamics and A factors for analogous isomerizations. The large difference in barrier heights coupled with almost an order of magnitude difference in A factors are evidently responsible for the results of the QRRK calculations which indicate that for 1 atm and 1100 K almost 100% of the products from the reaction of O atom with benzene are phenoxy radical and H atom.

The ratio shown in Table III with 100% phenoxy + H formation (reaction 4) was found to give the best comparison between the model and experiment. This observation agrees with the conclusions of Cvetanovic[23] and the QRRK calculations. When partial phenol formation was included in the model, the resulting reaction rate of benzene was much too slow.[14]

The reaction of O with phenol (reaction 12) has not been studied but, due to the lack of presence of dihydroxybenzene ($C_6H_4(OH)_2$), oxygen atom is presumed to abstract the H from the hydroxy group rather than add to the ring. The rate used was based on 1/6 of the rate of O abstracting an H from the side chain of xylene[21] which has six abstractable H's. The choice of this analogous reaction was based on the similarity in bond strengths and aromatic structure.

Because of the presence of vinyl and butadienyl radicals (discussed later), the abstraction of the hydroxyl H of phenol by these radicals was included as reactions 13 and 14. Both reactions are highly exothermic due to the large vinylic C–H bond strength of approximately 106 kcal/mol for the ethene and butadiene products compared to the 87 kcal/mol O–H bond in phenol. Because of this large driving force, the rate constant of reaction 9, which is also highly exothermic, was chosen as an estimate for

$$C_6H_5OH + OH \rightarrow C_6H_5O + H_2O \qquad (9)$$

reactions 13 and 14.

Cyclopentadienyl, C_5H_5, formed from reaction 7 is a resonantly stabilized radical and thus radical–radical reactions are expected to occur.[6,28] Because of the speed of radical–radical reactions, cyclopentadiene, C_5H_6, is formed mainly by H atom combination with cyclopentadienyl:

$$C_5H_5 + H \rightarrow C_5H_6 \qquad (16)$$

The estimated rate constant used for this reaction is slightly larger than that calculated by Dean[29] for 0.58 atm conditions, 6×10^{13} $cm^3/mol/s$. Reaction of cyclopentadiene is postulated to occur by abstraction of the weak H's (reactions 20–27). Addition of radicals to the ring was not included due to the presence of the easily abstractable H's (C–H bond energy of 74.4 kcal/mol).

The abstraction of an H by O_2 from cyclopentadiene (reaction 20) was included as a consumption route for cyclopentadiene, but not for phenol since the difference in H bond energies is enough

(23) Cvetanovic, R. J. *J. Phys. Chem. Ref. Data* **1987**, *16*(2), 261.
(24) Mulder, P.; Louw, R. *Int. J. Chem. Kinet.* **1988**, *20*, 577.
(25) Dean, A. M. *J. Phys. Chem.* **1985**, *89*, 4600.
(26) Westmoreland, P. R.; Howard, J. B.; Longwell, J. P.; Dean, A. M. *AIChE J.* **1986**, *32*, 12, 1971.
(27) Ritter, E. R.; Bozzelli, J. W.; Dean, A. M. *J. Phys. Chem.* **1990**, *94*, 2493.
(28) Bozzelli, J. W.; Desai, V.; Ritter, E. R. Mechanistic Considerations for Cyclopentadiene and Cyclopentadienyl Radical Conversion During Benzene Oxidation. Presented at the Spring Technical Meeting, Central States Section, Combust Inst., paper No. 19, 1990.
(29) Dean, A. M. *J. Phys. Chem.* **1990**, *94*, 1436.

TABLE III: Benzene Oxidation Submodel $k = AT^n \exp(-E_a/RT)$[a]

		rate constant parameters						
		forward			reverse			
no.	reaction	A	n	E_a	A	n	E_a	ref
1	$C_6H_5 + H = C_6H_6$	2.20E+14	0.00	0	3.32E+19	−0.85	111 900	53
2	$C_6H_6 + O_2 = C_6H_5 + HO_2$	6.30E+13	0.00	60 000	1.27E+09	0.75	−2 740	54
3	$C_6H_6 + OH = C_6H_5 + H_2O$	2.11E+13	0.00	4 570	9.72E+08	0.98	11 935	55
4	$C_6H_6 + O = C_6H_5O + H$	2.78E+13	0.00	4 910	7.57E+14	−0.46	20 350	21
5	$C_6H_6 + H = C_6H_5 + H_2$	2.50E+14	0.00	16 000	5.26E+08	1.16	7 737	56
6	$C_6H_5 + O_2 = C_6H_5O + O$	2.09E+12	0.00	7 470	5.91E+16	−1.10	15 565	57
7	$C_6H_5O = CO + C_5H_5$	2.51E+11	0.00	43 900	9.50E+03	1.40	26 550	37
8	$C_6H_5O + H = C_6H_5OH$	2.50E+14	0.00	0	1.23E+16	−0.26	86 430	39
9	$C_6H_5OH + OH = C_6H_5O + H_2O$	6.00E+12	0.00	0	8.47E+11	0.39	32 810	39
10	$C_6H_5OH + H = C_6H_6 + OH$	2.21E+13	0.00	7 910	3.54E+09	0.98	7 906	39
11	$C_6H_5OH + H = C_6H_5O + H_2$	1.15E+14	0.00	12 400	7.42E+11	0.57	29 590	39
12	$C_6H_5OH + O = C_6H_5O + OH$	2.81E+13	0.00	7 352	1.22E+11	0.52	22 782	est., see text
13	$C_2H_3 + C_6H_5OH = C_2H_4 + C_6H_5O$	6.00E+12	0.00	0	6.79E+14	−0.08	20 600	est., see text
14	$C_4H_5 + C_6H_5OH = C_4H_6 + C_6H_5O$	6.00E+12	0.00	0	4.48E+14	−0.13	20 430	est., see text
15	$C_6H_5 + C_6H_5OH = C_6H_6 + C_6H_5O$	4.91E+12	0.00	4 400	1.51E+16	−0.59	29 850	58
16	$C_5H_5 + H = C_5H_6$	1.00E+14	0.00	0	3.70E+13	0.56	74 580	est., see text
17	$C_5H_5 + O = C_4H_5 + CO$	1.00E+14	0.00	0	3.08E+04	1.76	57 320	est., see text
18	$C_5H_5 + HO_2 = C_5H_5O + OH$	3.00E+13	0.00	0	4.70E+14	−0.31	4 621	est., see text
19	$C_5H_5 + OH = C_5H_4OH + H$	3.00E+13	0.00	0	1.97E+16	−0.70	−964	est., see text
20	$C_5H_6 + O_2 = C_5H_5 + HO_2$	2.00E+13	0.00	25 000	1.64E+14	−0.67	−440	est., see text
21	$C_5H_6 + HO_2 = C_5H_5 + H_2O_2$	1.99E+12	0.00	11 660	2.54E+15	−1.06	24 980	est., see text
22	$C_5H_6 + OH = C_5H_5 + H_2O$	3.43E+09	1.18	−447	6.44E+10	0.74	44 213	est., see text
23	$C_5H_6 + H = C_5H_5 + H_2$	2.19E+08	1.77	3 000	1.88E+08	1.52	32 030	est., see text
24	$C_5H_6 + O = C_5H_5 + OH$	1.81E+13	0.00	3 080	1.05E+13	−0.30	30 360	est., see text
25	$C_5H_6 + C_2H_3 = C_5H_5 + C_2H_4$	6.00E+12	0.00	0	9.02E+16	−0.90	32 440	est., see text
26	$C_5H_6 + C_4H_5 = C_5H_5 + C_4H_6$	6.00E+12	0.00	0	5.96E+16	−0.95	32 280	est., see text
27	$C_5H_6 + C_6H_5O = C_5H_5 + C_6H_5OH$	3.16E+11	0.00	8 000	4.20E+13	−0.82	19 840	est., 32
28	$C_5H_5O = C_4H_5 + CO$	2.51E+11	0.00	43 900	2.40E−03	2.66	30 100	est. from reaction 7
29	$C_5H_4OH = C_5H_4O + H$	2.10E+13	0.00	48 000	4.03E+12	0.44	4 860	est., see text
30	$C_5H_4O = CO + C_2H_2 + C_2H_2$	1.00E+15	0.00	78 000	7.14E−05	3.59	−4 360	est., see text
31	$C_4H_5 = C_2H_3 + C_2H_2$	3.98E+11	0.70	42 260	1.02E+03	2.55	480	50
32	$C_4H_5 + M = C_4H_4 + H + M$	2.98E+33	−5.00	44 320	1.48E+31	−4.46	−1 470	est. from reaction 34
33	$C_4H_5 + O_2 = C_4H_4 + HO_2$	1.20E+11	0.00	0	1.81E+09	0.44	3 350	est. from reaction 35
34	$C_2H_3 + M = C_2H_2 + H + M$	2.98E+33	−5.00	44 320	7.27E+33	−5.02	4 170	*b*
35	$C_2H_3 + O_2 = C_2H_2 + HO_2$	1.20E+11	0.00	0	8.90E+11	−0.13	8 995	30
36	$C_2H_2 + O = HCCO + H$	5.80E+06	2.09	1 562	4.34E+06	1.94	20 422	59
37	$C_2H_2 + O = CH_2 + CO$	1.40E+06	2.09	1 562	1.25E+00	3.54	47 992	59
38	$CH_2 + O_2 = H + OH + CO$	6.02E+11	0.00	0	1.39E+10	0.39	57 090	*c*
39	$CH_2 + O_2 = CO + H_2O$	2.41E+11	0.00	0	3.87E+10	0.51	176 300	*c*
40	$HCCO + O_2 = OH + CO + CO$	1.46E+12	0.00	2 500	4.02E+04	1.98	87 150	60
41	$H + O_2 = O + OH$	1.91E+14	0.00	16 440	2.81E+11	0.47	−920	36
42	$O + H_2 = H + OH$	5.13E+04	2.67	6 290	3.46E+04	2.62	4 536	36
43	$H_2 + OH = H_2O + H$	2.14E+08	1.51	3 430	4.68E+09	1.32	19 060	36
44	$OH + OH = O + H_2O$	1.23E+04	2.62	−1 878	3.99E+05	2.48	15 502	36
45	$H_2 + M = H + H + M$	4.57E+19	−1.40	104 400	1.44E+20	−1.71	800	36
46	$O + O + M = O_2 + M$	6.17E+15	−0.50	0	8.95E+17	−0.71	119 200	36
47	$O + H + M = OH + M$	4.68E+18	−1.00	0	1.00E+18	−0.74	101 900	36
48	$H + OH + M = H_2O + M$	2.24E+22	−2.00	0	1.56E+23	−1.88	119 200	36
49	$H + O_2 + M = HO_2 + M$	6.76E+19	−1.42	0	2.05E+20	−1.52	49 140	36
50	$H + HO_2 = H_2 + O_2$	6.61E+13	0.00	2 130	6.92E+12	0.42	56 600	36
51	$H + HO_2 = OH + OH$	1.70E+14	0.00	870	1.78E+10	0.84	36 230	36
52	$HO_2 + O = O_2 + OH$	1.74E+13	0.00	−400	1.23E+12	0.37	52 320	36
53	$HO_2 + OH = H_2O + O_2$	1.44E+16	−1.00	0	3.13E+16	−0.77	70 100	36
54	$HO_2 + HO_2 = H_2O_2 + O_2$	3.02E+12	0.00	1 390	4.72E+14	−0.39	40 160	36
55	$H_2O_2 + M = OH + OH + M$	1.20E+17	0.00	45 500	2.66E+10	1.34	−7 050	36
56	$H_2O_2 + H = H_2O + OH$	1.00E+13	0.00	3 590	1.54E+07	1.46	70 280	36
57	$H_2O_2 + H = HO_2 + H_2$	4.79E+13	0.00	7 950	3.21E+10	0.81	23 660	36
58	$H_2O_2 + O = OH + HO_2$	9.55E+06	2.00	3 970	4.33E+03	2.76	17 920	36
59	$H_2O_2 + OH = H_2O + HO_2$	7.08E+12	0.00	1 430	1.04E+11	0.62	32 760	36
60	$CO + O + M = CO_2 + M$	2.51E+13	0.00	−4 540	4.94E+19	−1.08	123 560	36
61	$CO + O_2 = CO_2 + O$	2.51E+12	0.00	47 690	3.41E+16	−0.87	56 569	36
62	$CO + OH = CO_2 + H$	1.50E+07	1.30	−765	1.38E+14	−0.04	25 475	36
63	$CO + HO_2 = CO_2 + OH$	6.03E+13	0.00	22 950	5.78E+16	−0.50	84 550	36
64	$HCO + M = H + CO + M$	1.86E+17	−1.00	17 000	1.28E+16	−0.64	1 340	36
65	$HCO + O_2 = CO + HO_2$	4.17E+12	0.00	0	8.68E+11	0.26	33 480	36
66	$HCO + H = CO + H_2$	7.24E+13	0.00	0	1.58E+12	0.68	87 950	36
67	$HCO + O = CO + OH$	3.02E+13	0.00	0	4.45E+11	0.62	86 200	36
68	$HCO + OH = CO + H_2O$	3.02E+13	0.00	0	1.44E+13	0.49	103 600	36

[a] Units: cm^3, moles, seconds, calories, kelvin. In this and all tables E + $n \equiv \times 10^n$. [b] Forward rate constant is a fit to the value recommended by Tsang and Hampson.[30] [c] CH_2 reaction rate constants are triplet values recommended by Tsang and Hampson.[30]

to make the phenol reaction too slow to be important. The rate constant for reaction 20 was estimated by using the preexponential factor for oxygen abstracting an H from formaldehyde[30] and by estimating the activation energy as being equal to the endo-

TABLE IV: Toluene Oxidation Model $k = AT^n \exp(-E_a/RT)$[a]

no.	reaction	rate constant parameters: forward A	forward n	forward E_a	reverse A	reverse n	reverse E_a	ref
69	$C_6H_5CH_2 + H = C_6H_5CH_3$	1.80E+14	0.00	0	8.79E+14	0.37	90840	17, 61
70	$C_6H_5CH_3 = C_6H_5 + CH_3$	1.40E+16	0.00	99800	1.17E+06	1.96	−3700	62
71	$C_6H_5CH_3 + O_2 = C_6H_5CH_2 + HO_2$	3.00E+14	0.00	41400	1.86E+14	−0.48	−300	est., see text
72	$C_6H_5CH_3 + OH = C_6H_5CH_2 + H_2O$	1.26E+13	0.00	2583	6.95E+12	−0.02	33300	63
73	$C_6H_5CH_3 + H = C_6H_5CH_2 + H_2$	1.20E+14	0.00	8235	1.31E+12	0.27	23070	64
74	$C_6H_5CH_3 + H = C_6H_6 + CH_3$	1.20E+13	0.00	5148	1.20E+12	0.00	15970	64
75	$C_6H_5CH_3 + O = OC_6H_4CH_3 + H$	1.63E+13	0.00	3418	7.49E+17	−1.01	19060	21
76	$CH_3 + C_6H_5CH_3 = CH_4 + C_6H_5CH_2$	3.16E+11	0.00	9500	3.10E+13	−0.42	27000	65
77	$C_6H_5 + C_6H_5CH_3 = C_6H_6 + C_6H_5CH_2$	2.10E+12	0.00	4400	4.09E+16	−1.06	27910	58
78	$C_6H_5OH + C_6H_5CH_2 = C_6H_5O + C_6H_5CH_3$	1.05E+11	0.00	9500	1.04E+10	0.63	13912	est. from reaction 76
79	$HOC_6H_4CH_3 + C_6H_5CH_2 = OC_6H_4CH_3 + C_6H_5CH_3$	1.05E+11	0.00	9500	8.47E+10	0.61	13650	est. from reaction 76
80	$C_6H_5CH_2 + O = C_6H_5CHO + H$	2.50E+14	0.00	0	5.59E+14	0.24	66600	est., see text
81	$C_6H_5CH_2 + O = C_6H_5 + CH_2O$	8.00E+13	0.00	0	8.79E+06	1.98	58100	est., see text
82	$C_6H_5CH_2 + HO_2 = C_6H_5CHO + H + OH$	2.50E+14	0.00	0	2.72E+11	0.82	104	est., see text
83	$C_6H_5CH_2 + HO_2 = C_6H_5 + CH_2O + OH$	8.00E+13	0.00	0	4.28E+03	2.55	−8399	est., see text
84	$C_6H_5CH_2 + C_6H_5CH_2 =$ bibenzyl	2.51E+11	0.40	0	1.38E+18	−0.50	67170	66
85	$C_6H_5C_2H_5 = C_6H_5CH_2 + CH_3$	2.00E+15	0.00	72700	9.05E+06	1.49	−7160	67
86	$C_6H_5CH_2 + OH = C_6H_5CH_2OH$	6.00E+13	0.00	0	3.77E+18	−0.59	84820	est., see text
87	$C_6H_5CH_2OH + O_2 = C_6H_5CHO + HO_2 + H$	2.00E+14	0.00	41400	1.01E+11	0.47	−29540	est. from reaction 71
88	$C_6H_5CH_2OH + OH = C_6H_5CHO + H_2O + H$	8.43E+12	0.00	2583	9.73E+09	0.69	1748	est. from reaction 72
89	$C_6H_5CH_2OH + H = C_6H_5CHO + H_2 + H$	8.00E+13	0.00	8235	4.22E+09	0.88	−8225	est. from reaction 73
90	$C_6H_5CH_2OH + H = C_6H_6 + CH_2OH$	1.20E+13	0.00	5148	1.95E+08	0.98	16640	est. from reaction 74
91	$C_6H_5CH_2OH + C_6H_5CH_2 = C_6H_5CHO + C_6H_5CH_3 + H$	2.11E+11	0.00	9500	2.72E+08	0.77	−22210	est. from reaction 76
92	$C_6H_5CH_2OH + C_6H_5 = C_6H_5CHO + C_6H_6 + H$	1.40E+12	0.00	4400	3.51E+13	−0.28	−3800	est. from reaction 77
93	$C_6H_5CHO + O_2 = C_6H_5CO + HO_2$	1.02E+13	0.00	38950	3.39E+10	0.22	900	*b*
94	$C_6H_5CHO + OH = C_6H_5CO + H_2O$	1.71E+09	1.18	−447	1.25E+07	1.64	31080	est. from reaction 126
95	$C_6H_5CHO + H = C_6H_5CO + H_2$	5.00E+13	0.00	4928	1.67E+10	0.64	20840	est. from reaction 128
96	$C_6H_5CHO + H = C_6H_6 + HCO$	1.20E+13	0.00	5148	1.08E+08	1.19	17550	est. from reaction 74
97	$C_6H_5CHO + O = C_6H_5CO + OH$	9.04E+12	0.00	3080	2.04E+09	0.59	17230	est. from reaction 127
98	$C_6H_5CH_2 + C_6H_5CHO = C_6H_5CH_3 + C_6H_5CO$	2.77E+03	2.81	5773	2.26E+01	3.35	6437	est. from reaction 130
99	$CH_3 + C_6H_5CHO = CH_4 + C_6H_5CO$	2.77E+03	2.81	5773	2.22E+03	2.93	23930	est. from reaction 130
100	$C_6H_5 + C_6H_5CHO = C_6H_6 + C_6H_5CO$	7.01E+11	0.00	4400	1.11E+14	−0.52	28570	est. from reaction 77
101	$C_6H_5C_2H_5 + OH = C_6H_5C_2H_3 + H_2O + H$	8.43E+12	0.00	2583	2.21E+09	0.83	−11850	est. from reaction 72
102	$C_6H_5C_2H_5 + H = C_6H_5C_2H_3 + H_2 + H$	8.00E+13	0.00	8235	9.57E+08	1.01	−21820	est. from reaction 73
103	$C_6H_5C_2H_5 + O_2 = C_6H_5C_2H_3 + HO_2 + H$	2.00E+14	0.00	41400	2.28E+10	0.60	−43140	est. from reaction 71
104	$OC_6H_4CH_3 + H = HOC_6H_4CH_3$	2.50E+14	0.00	0	1.51E+15	−0.23	86690	39
105	$OC_6H_4CH_3 = C_6H_6 + H + CO$	2.51E+11	0.00	43900	1.55E+00	2.44	760	37, see text
106	$HOC_6H_4CH_3 + OH = OC_6H_4CH_3 + H_2O$	6.00E+12	0.00	0	6.88E+12	0.36	32550	39
107	$HOC_6H_4CH_3 + H = OC_6H_4CH_3 + H_2$	1.15E+14	0.00	12400	6.03E+12	0.55	29330	39
108	$HOC_6H_4CH_3 + H = C_6H_5CH_3 + OH$	2.21E+13	0.00	7910	1.70E+07	1.51	7438	39
109	$HOC_6H_4CH_3 + H = C_6H_5OH + CH_3$	1.20E+13	0.00	5148	7.27E+05	1.64	13090	est. from reaction 74
110	$C_6H_5CO = C_6H_5 + CO$	3.98E+14	0.00	29400	1.56E+06	2.08	1970	68
111	$CH_4 = CH_3 + H$	6.14E+14	0.00	103800	5.35E+12	0.00	−1187	69
112	$CH_4 + H = CH_3 + H_2$	5.47E+07	1.97	11210	1.64E+06	1.97	10170	69
113	$CH_4 + OH = CH_3 + H_2O$	5.72E+06	1.96	2639	8.09E+05	1.96	16790	69
114	$CH_4 + O = CH_3 + OH$	6.93E+08	1.56	8484	9.31E+06	1.56	5589	69
115	$CH_4 + HO_2 = CH_3 + H_2O_2$	1.81E+11	0.00	18580	2.43E+12	−0.66	1003	70
116	$CH_3 + HO_2 = CH_3O + OH$	2.00E+13	0.00	1076	1.01E+14	0.00	25380	69
117	$CH_3 + OH = CH_2OH + H$	1.09E+11	0.40	−708	9.48E+14	−0.60	−3772	69
118	$CH_3 + O = CH_2O + H$	8.43E+13	0.00	0	4.12E+15	−0.15	70270	69
119	$CH_3 + O_2 = CH_3O + O$	1.99E+18	−1.57	29230	6.15E+19	−1.83	1082	70
120	$HCO + CH_3 = CH_4 + CO$	1.20E+14	0.00	0	5.42E+14	0.45	89480	70
121	$CH_3 + HO_2 = CH_4 + O_2$	3.61E+12	0.00	0	4.08E+13	0.00	55330	69
122	$CH_3O + M = CH_2O + H + M$	9.37E+24	−2.70	30590	5.62E+23	−2.58	10280	69
123	$CH_3O + O_2 = CH_2O + HO_2$	6.30E+10	0.00	2600	7.07E+08	0.36	30620	69
124	$CH_2OH + O_2 = CH_2O + HO_2$	2.41E+14	0.00	5000	7.85E+12	0.61	25860	69
125	$CH_2OH + M = CH_2O + H + M$	1.67E+24	−2.50	34190	1.27E+23	−2.03	5990	69
126	$CH_2O + OH = HCO + H_2O$	3.43E+09	1.18	−447	1.38E+08	1.42	28260	69
127	$CH_2O + O = HCO + OH$	1.81E+13	0.00	3080	8.22E+10	0.22	14780	69
128	$CH_2O + H = HCO + H_2$	1.00E+14	0.00	4928	8.73E+11	0.24	18460	69
129	$CH_2O + HO_2 = HCO + H_2O_2$	1.99E+12	0.00	11660	7.96E+12	−0.42	8659	69
130	$CH_2O + CH_3 = HCO + CH_4$	5.54E+03	2.81	5863	1.65E+03	3.05	20430	69

[a] Units: cm^3, moles, seconds, calories, kelvin. [b] Rate constant estimated from $O_2 + CH_2O \rightarrow HCO + HO_2$, Tsang and Hampson.[30]

thermicity of the reaction. The rate constants of the abstraction of H from cyclopentadiene by HO_2, OH, H, and O were each estimated using the analogous exothermic reactions with formaldehyde.[30] The rate constants of vinyl and butadienyl abstracting H from cyclopentadiene (reactions 25 and 26) were estimated to be equal to the rate constants for reactions 13 and 14.

The oxidation mechanism of cyclopentadienyl is postulated to occur through the reactions outlined by Brezinsky[6] (Figure 2). The addition of O atom to cyclopentadienyl (reaction 17) is expected to lead to the formation of the energized cyclic adduct $[C_5H_5O]^*$. This adduct can decompose to form butadienyl and CO after ring opening and a hydrogen transfer in the C_4 radical species:[28]

$$C_5H_5 + O \rightarrow [C_5H_5O]^* \rightarrow C_4H_5 + CO \qquad (17)$$

(30) Tsang, W.; Hampson, R. F. *J. Phys. Chem. Ref. Data* **1986**, *15*, 1087.

The overall rate constant of reaction 17 was estimated to be 1×10^{14} cm^3/mol/s. Because this rate constant is near the collision frequency, there is an implicit assumption that the $[C_5H_5O]^*$ adduct decomposes through the exothermic channel to products at a rate much faster than the reverse rate to re-form the reactants. The loss of an H atom from the $[C_5H_5O]^*$ adduct to form the cyclic ketone C_5H_4O plus H atom ($\Delta H_r = -58$ kcal/mol) was also considered but was not used since reaction 17 explains the experimental detection of butadiene as discussed below.

By analogy with the reaction of HO_2 with benzyl,[5,17] the peroxide adduct, $[C_5H_5OOH]^*$, formed from reaction 18 is expected to lose OH to form C_5H_5O:

$$C_5H_5 + HO_2 \rightarrow [C_5H_5OOH]^* \rightarrow C_5H_5O + OH \quad (18)$$

The rate constant for reaction 18, a radical–radical reaction, was estimated to be 3×10^{13} cm^3/mol/s to account for some contribution from the reverse decomposition of the adduct. The C_5H_5O formed then decomposes unimolecularly to butadienyl and CO (reaction 28).

Addition of OH to cyclopentadienyl is modeled as reaction 19

$$C_5H_5 + OH \rightarrow [C_5H_5OH]^* \rightarrow C_5H_4OH + H \quad (19)$$

This reaction is nearly thermoneutral and hence the reverse reaction can occur readily. On the basis of the experimental observation of a lack of hydroxycyclopentadiene (C_5H_5OH), thermalization of the $[C_5H_5OH]^*$ adduct is not expected to occur to a significant extent. Loss of the H from the oxygen, instead of from the ring, was considered; however, a reaction to break the O–H bond would be highly endothermic ($H_r = +31$ kcal/mol) and slow. The rate constant for reaction 19 was estimated to be the same as for reaction 18 which is again lower than the collision frequency to account for back decomposition of the energized adduct.

Analogous to the decomposition of hydroxymethyl (CH_2OH) to formaldehyde and H, the C_5H_4OH product from reaction 19 can decompose unimolecularly:

$$C_5H_4OH \rightarrow C_5H_4O + H \quad (29)$$

The rate for reaction 29 was estimated using the methods of Benson,[32] details of which can be found in the thesis of Emdee.[14] The cyclic ketone formed is then postulated to open and lose the CO group to form two acetylenes:

$$C_5H_4O \rightarrow CO + 2C_2H_2 \quad (30)$$

The formation of vinylacetylene was considered but, from the discussion of Benson,[33] the more exothermic path to acetylene formation was chosen. The rate for reaction 30 was given an appropriate activation energy to reflect the endothermicity, while the A factor was estimated from the A factors for pyrolysis of ring compounds discussed in Benson.[32]

(ii) Comparison of the Model and Experimental Data. The flow reactor experiments approximate an adiabatic, constant pressure, reaction system in which hydrodynamic and diffusional transport effects are small compared to changes brought about by chemical reaction. Thus, to make a comparison between the experimental data and the kinetic model, the reaction system was numerically treated as a zero-dimensional, adiabatic, constant pressure, homogeneous mixture using CHEMKIN.[34] However, the large-scale turbulent mixing in the diffuser section of the flow reactor accelerates the initial consumption of the fuel due to the enhanced eddy diffusion of radicals. Indeed, the present experimental data, as well as the data of previous investigators, indicate that substantially more fuel is consumed in the diffuser section than can be explained by zero dimensional, homogeneous mixture reaction rates. From the modeling work performed here, the effects of the initial perturbations of the radical pool caused by mixing are quickly damped out due to fast radical reactions. After the perturbation disappears, the radical pool returns to the near-steady-state values of the unperturbed model as does the rate of the fuel decay. Thus the mixing of fuel and oxidizer is not expected to alter the kinetics significantly but is responsible for the shortened chemical induction time for fuel consumption. Consequently, the experimentally derived reaction time is only relative. Thus the comparison between experiment and model was made after the experimental data were shifted in time so that the experimental fuel concentration at 50% of the measured consumption matched the model prediction. The time shift was constant for each experimental condition.

The experimental data and model results for benzene are compared in Figure 3. Intermediate species profiles are shown in Figure 4 for case 2 (see Table I) only; further results for other conditions can be found in the thesis of Emdee.[14]

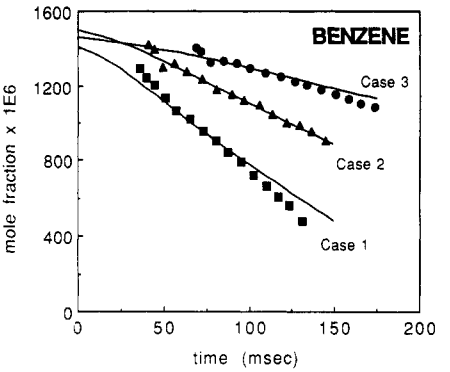

Figure 3. Experimental (symbols) and model (lines) benzene decay profiles. The experimental data for cases 1, 2, and 3 were shifted in time by +33, +37, and +68 ms, respectively; see text for further discussion.

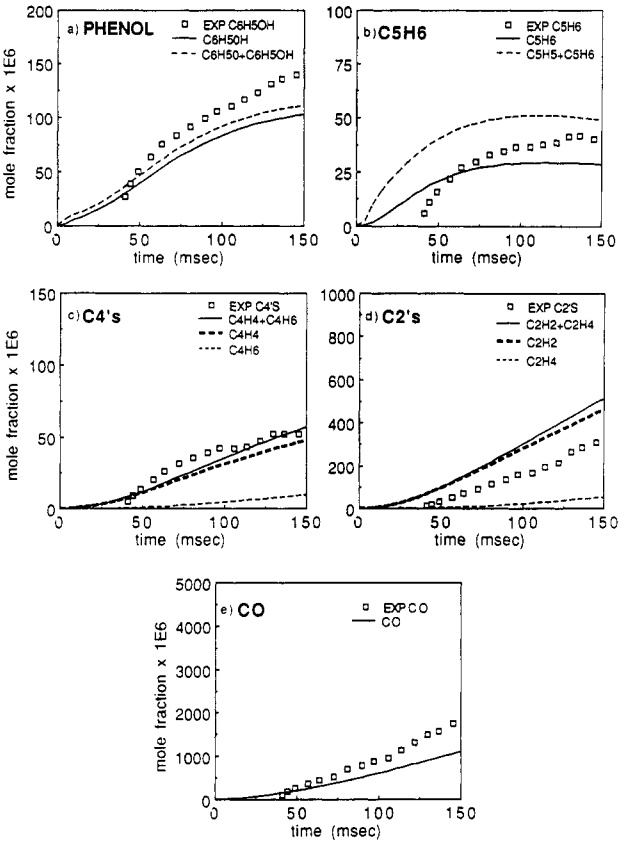

Figure 4. Experimental (symbols) and model predicted (lines) intermediate species profiles for case 2.

(31) McMillen, D. F.; Golden, D. M. *Annu. Rev. Phys. Chem.* **1982**, *33*, 493.

(32) Benson, S. W. *Thermochemical Kinetics*, 2nd ed.; Wiley: New York, 1976.

(33) Benson, S. W. *Int. J. Chem. Kinet.* **1989**, *21*, 233.

(34) Kee, R. J.; Miller, J. A.; Jefferson, T. H. CHEMKIN: A General Purpose, Problem-Independent, Transportable, Fortran Chemical Kinetics Code Package. Sandia Natl. Lab. Report SAND80-8003, 1980.

The model prediction of the fuel decay was in good agreement with the experimental data for all three conditions considered. A fair match was achieved between the total C_4 and C_2 species. Lovell et al.[13] did not make a distinction between the C_4's and the C_2's. However, they did indicate that the C_4's were vinylacetylene (C_4H_4) and butadiene (C_4H_6) in about a 3:1 ratio, and the C_2's were "predominantly acetylene and some ethylene". Because the present model can distinguish between species, the individual components of the C_4's and C_2's are also plotted in Figure 4. The vinylacetylene to butadiene ratio appears similar to the ratio indicated by Lovell et al.[13] and the acetylene mole fraction is much larger than the ethylene mole fraction.

The mole fractions of phenoxy and cyclopentadienyl are included in the comparisons of phenol and cyclopentadiene because these species are resonantly stable and might be expected to build up to relatively high concentrations. If these radical species found a source of H in the sampling probe, they would have been detected as the stable parent species. Figure 4 shows that the inclusion of these radicals in the total phenol and cyclopentadiene profiles has a small effect on the former and a large effect on the latter.

Although good agreement between the predicted and experimental phenol profiles was achieved for the lean and near stoichiometric conditions (cases 1 and 2), the model tended to underpredict the phenol mole fractions for rich conditions (case 3). The cyclopentadiene profiles were predicted with fair agreement by the total of the C_5H_6 and C_5H_5 concentrations for the lean and near-stoichiometric conditions but was overpredicted by the rich condition. The overprediction of the cyclopentadiene coupled with the underprediction of the phenol for case 3 suggests that the phenol is being consumed too quickly for this case. The CO was underpredicted for all equivalence ratios considered which in part reflects the lack of a full submechanism for small molecule chemistry.

(iii) Reaction Path Analysis. An analysis of the flux through each reaction revealed the following:

1. The main routes for fuel consumption are through reactions 3 and 4, with reaction 3 being more important toward the end

$$C_6H_6 + OH \rightarrow C_6H_5 + H_2O \quad (3)$$

$$C_6H_6 + O \rightarrow C_6H_5O + H \quad (4)$$

of the reaction sequence.

2. The production of phenol occurs mainly through reaction 8

$$C_6H_5O + H \rightarrow C_6H_5OH \quad (8)$$

and reaction 9 is the primary consuming reaction.

$$C_6H_5OH + OH \rightarrow C_6H_5O + H_2O \quad (9)$$

3. Reaction 16 is almost the sole source of cyclopentadiene.

$$C_5H_5 + H \rightarrow C_5H_6 \quad (16)$$

The main removal path for cyclopentadiene is through reaction 20.

$$C_5H_6 + O_2 \rightarrow C_5H_5 + HO_2 \quad (20)$$

Because cyclopentadiene is formed from the cyclopentadienyl radical and then reacts further to produce this same radical, cyclopentadiene serves only as a diversion in the path from reactants to products. Furthermore, the strong presence of reaction 16 indicates that cyclopentadienyl acts as a sink for H atoms in the system. These observations apply to phenol and phenoxy as well. Phenol is formed from phenoxy by recombination with H atoms and is consumed to form phenoxy again. One can conclude that, because H atoms are important to the formation of the radical pool, resonantly stable species such as cyclopentadienyl and phenoxy tend to inhibit the reaction system.

(iv) Sensitivity Analysis. A linear sensitivity analysis was performed using CHEMSEN[35] to determine how sensitive the model

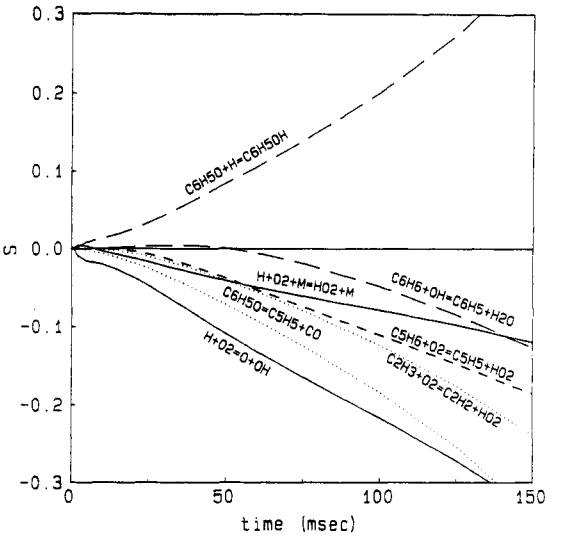

Figure 5. Linear sensitivity coefficients, S, for reactions that affect the benzene species profile for case 2.

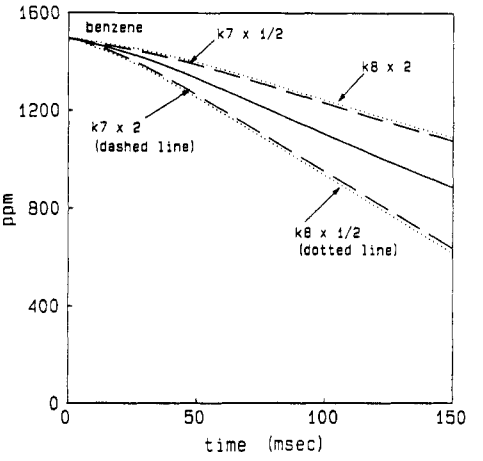

Figure 6. Model predictions for case 2 showing the sensitivity of the benzene profile to the rate constants for reaction 7 $C_6H_5O \rightarrow C_5H_5 + CO$ and reaction 8 $C_6H_5O + H \rightarrow C_6H_5OH$.

is to changes in the reaction rates. The sensitivity coefficients are given as

$$S = \frac{d[X]/[X]}{dk/k}$$

where S represents the percent change in species concentration, $d[X]/[X]$, for each percent change in the rate constant, dk/k.

Figure 5 shows a plot of the sensitivity coefficients for the most sensitive reactions that affect the benzene profile. The three most sensitive are

$$H + O_2 \rightarrow O + OH \quad (41)$$

$$C_6H_5O \rightarrow C_5H_5 + CO \quad (7)$$

$$C_6H_5O + H \rightarrow C_6H_5OH \quad (8)$$

The first reaction has been studied by many investigators and the rate recommended by Yetter et al.[36] is uncertain by a factor of 2. Because the Yetter et al.[36] $H_2/O_2/CO$ submechanism was verified over much wider conditions than this model, the recommended value for the $H+O_2$ reaction was not considered further. The latter two reactions determine the fate of the phenoxy radical. Because the fuel must pass through the phenoxy radical to reach the final products, the fate of this radical is very important.

The rate of reaction 7 was determined by Lin and Lin[37] from 1000 to 1580 K and 0.4 to 0.9 atm and has an uncertainty factor

(35) Kramer, M. A.; Kee, R. J.; Rabitz, H. CHEMSEN: A Computer Code for Sensitivity Analysis of Elementary Chemical Kinetic Models; Sandia Natl. Lab. Report SAND 82-8230, 1982.

(36) Yetter, R. A.; Dryer, F. L.; Rabitz, H. *Combust. Sci. Technol. J.* **1991**, *79*, 97.

(37) Lin, C.-Y.; Lin, M. C. *J. Phys. Chem.* **1986**, *90*, 425.

of 2. The effects of this uncertainty are shown in Figure 6 for the benzene profile. Ritter et al.,[38] in preliminary modeling work, have recently questioned the decomposition rate of reaction 7, suggesting Lin and Lin's[37] rate constant may be too high by about a factor of 1000 depending on temperature. Such a drastic difference in rate constants determined by these two investigators and the model sensitivity to this reaction necessitates further measurements. The model presented here seems to support Lin and Lin's[37] value. Also shown in Figure 6 are the model results obtained when the rate of reaction 8 is varied by a factor of 2. This rate was determined by He et al.[39] and is suggested to be accurate to within 25%. Figure 6 demonstrates how sensitive the model is to the rate constants for reactions 7 and 8 and is certainly an argument for continued investigation of these two reactions.

Despite the success of the benzene submodel in predicting experimental data, there are some difficulties. For example, it was estimated that abstraction of the weakly bonded H's of cyclopentadiene would be faster than addition of radicals to the ring and thus addition reactions such as those suggested by Bozzelli et al.[28] were not included. The effect of including such reactions needs to be studied in further work. One must also be aware that the rate constants of the radical–radical reactions involving cyclopentadienyl radical (reactions 16–19) were estimated. As a result, these rates have large uncertainties. The sensitivity analysis did show however that the fuel decay was not very sensitive to the rate constants used.

The build up of the cyclic ketone C_5H_4O (reaction 29) should also be mentioned. This species is assumed to decompose solely by unimolecular ring opening to CO and two C_2H_2's (reaction 30). Because this is a very endothermic reaction, it is slow and the modeled level of C_5H_4O builds up to 50 ppm toward the end of the reaction sequence. This species was not a detected product in the experiments. Most likely, other reactions that consume C_5H_4O are occurring and have not been considered. The oxidation of cyclopentadiene is being studied in this laboratory and will be very helpful in making this part of the model more complete.

Despite the uncertainty in the C_5 submechanism of the benzene model, the results are satisfactory. With a good representation of the reaction of benzene through oxidation reactions, the oxidation of toluene was modeled.

B. Toluene Model. (i) Discussion of Reactions. The rate constant for reaction 71 was initially estimated and then adjusted

$$C_6H_5CH_3 + O_2 \rightarrow C_6H_5CH_2 + HO_2 \qquad (71)$$

for a better fit to the data. No direct determination of this rate is available in the literature, although estimates based on modeling were made by Bittker[10] and McLain et al.[9] Reaction 71 was not included in the earlier mechanism represented by Figure 2 because it was thought to be a minor reaction; as will be indicated later, it is very important to the reaction mechanism.

The rate constant for the reaction

$$C_6H_5CH_3 + O \rightarrow OC_6H_4CH_3 + H \qquad (75)$$

was taken from the work of Nicovich et al.[21] Although Nicovich et al.[21] did not perform a direct product analysis, the invariance of the rate constant to isotopic labeling of the methyl side chain permitted them to conclude that O atoms reacted with the aromatic ring and did not abstract a methyl side chain hydrogen. The increased reactivity of toluene with O atom compared to the measured reactivity of benzene and O atom led them to conclude that the reaction occurred through an electrophilic addition of the O atom to the ring augmented by the electron-donating characteristics of the methyl group. This result was consistent with other studies of electrophilic addition to aromatic rings[21,40] and implies that the ortho and para ring sites were favored over the meta and methyl attachment sites. The electrophilic addition of O atom to the ortho or para sites would lead to the production of either cresol or cresoxy radical in a process similar to the formation of either phenol or phenoxy radical in the reaction of O atom with benzene. The products of the reaction of O atom and toluene are postulated to be cresoxy and H atom, consistent as well with the postulated products of the analogous benzene and O atom reaction.

Reactions 80–86 describe benzyl radical–radical reactions. The reaction between benzyl and O_2 to form benzoxy

$$C_6H_5CH_2 + O_2 \rightarrow C_6H_5CH_2O + O$$

was originally included in the model but later dropped. Several studies[5,41,42] have indicated that this reaction, proceeding through an activated complex, is highly reversible at high temperatures. In fact, an estimated rate constant for this reaction[5] showed that this reaction is much slower than the radical–radical reactions listed below.

The reaction between O atom and benzyl was studied experimentally at room temperature and 1.5 mbar by Bartels et al.[43] These investigators suggested two reaction paths:

$$C_6H_5CH_2 + O \rightarrow [C_6H_5CH_2O]^* \rightarrow C_6H_5CHO + H \qquad (80)$$

$$C_6H_5CH_2 + O \rightarrow [C_6H_5CH_2O]^* \rightarrow C_6H_6 + HCO \qquad (81a)$$

The latter reaction would have to involve a 1,2 hydrogen shift in the activated benzoxy. QRRK calculations[26] for which the high-pressure Arrhenius A and E_{act} parameters for decomposition of the adduct are 2.0×10^{13} and 17.4 kcal/mol for reaction 80 and 1.0×10^{14} and 25.1 kcal/mol for reaction 81a indicate that the latter reaction appears to be much slower than reaction 80 at both flow reactor conditions and the conditions of Bartels'[43] experiments. Furthermore, the calculations indicate that the rates of reactions 80 and 81

$$C_6H_5CH_2 + O \rightarrow [C_6H_5CH_2O]^* \rightarrow C_6H_5 + CH_2O \qquad (81)$$

are competitive with very little decomposition to reactants. Both reactions 80 and 81 are β-scission decomposition reactions and would be expected to be faster than the hydrogen shift reaction (reaction 81a). It is possible that Bartels'[43] observation of benzene, which was thought to come from reaction 81a, is actually a result of secondary reactions between the phenyl and formaldehyde of reaction 81.

The branching ratio for the O + $C_6H_5CH_2$ reactions was set at 3 to 1 favoring benzaldehyde formation in order to best fit the experimental benzaldehyde data. Hippler et al.[42] also seem to prefer reaction 80 over reactions 81 and 81a in their 1200–1500 K benzyl oxidation model. They use a rate constant slightly higher than that given by Bartels et al.[43] Because the QRRK calculations indicate that the rate constant and branching ratio have no pressure dependence and very little temperature dependence, the overall O + $C_6H_5CH_2$ rate constant was taken to be that measured by Bartels et al.[43]

Other QRRK calculations show that the reaction between HO_2 and benzyl produces an energized benzyl peroxide which decomposes mainly to benzoxy and OH before stabilization or decomposition to reactants can take place (reactions 82 and 83). The benzoxy then undergoes the same reactions as the excited benzoxy in reactions 80 and 81:

$$C_6H_5CH_2 + HO_2 \rightarrow [C_6H_5CH_2OOH]^* \rightarrow C_6H_5CH_2O + OH \rightarrow C_6H_5CHO + H + OH \qquad (82)$$

$$\rightarrow C_6H_5 + CH_2O + OH \qquad (83)$$

A rate constant of 5×10^{12} cm^3/mol/s is recommended by Hippler et al.[42] for the total HO_2 + $C_6H_5CH_2$ reaction rate.

(38) Ritter, E. R.; Desai, V.; Bozzelli, J. W. Mechanism for Cyclopentadienyl Radical and Cyclopentadiene Conversion During Benzene Oxidation. Poster 42 presented at the *Symp. (Int.) Combust., 23*, 1990.

(39) He, Y. Z.; Mallard, W. G.; Tsang, W. *J. Phys. Chem.* **1988**, *92*, 2196.

(40) Ravishankara, A. R.; Wagner, S.; Fischer, S.; Smith, G.; Schiff, R.; Watson, T.; Testi, G.; Davis, D. D. *Int. J. Chem. Kinet.* **1976**, *10*, 783.

(41) Benson, S. W. *J. Am. Chem. Soc.* **1965**, *87*, 972.

(42) Hippler, H.; Reihs, C.; Troe, J. *Twenty-Third Symposium (International) Combustion [Proceedings]*; The Combustion Institute: Pittsburgh, 1991; p 37.

(43) Bartels, M.; Edelbattel-Einhaus, J.; Hoyermann, K. *Twenty-Second Symposium (International) Combustion [Proceedings]*; The Combustion Institute: Pittsburgh, 1989; p 1041.

Hippler et al.[42] stated that their value is derived from a fit between the model and the data and is not independent of the other rates derived in that work. Consequently, the value of 3.3×10^{14} $cm^3/mol/s$, albeit a high one, was chosen for the total reaction rate constant because of the similarity of this reaction to that of oxygen atom with benzyl radical which was measured by Bartels et al.[43]

The formation of benzyl alcohol was taken into account by reaction 86. There are no measured rate constants for this

$$C_6H_5CH_2 + OH \rightarrow C_6H_5CH_2OH \qquad (86)$$

reaction, although Hippler et al.[42] reported a value of 2×10^{13} $cm^3/mol/s$ based on their modeling work. Using this value as a starting point, the rate constant was increased by a factor of 3 to achieve the best fit between the model and the benzyl alcohol profiles.

The reactions of benzyl alcohol included abstraction of a benzylic H by a radical or O_2 and subsequent decomposition to benzaldehyde and H:

$$C_6H_5CH_2OH + X \rightarrow C_6H_5CHOH + XH \rightarrow C_6H_5CHO + H + XH \quad (87\text{–}89, 91, 92)$$

The intermediate formation of C_6H_5CHOH was not included as a separate reaction since the decomposition of this radical to benzaldehyde[7,42] is expected to be the only decomposition channel and should be fast relative to the abstraction rate. Reaction of ethylbenzene was taken into account by homolysis of the methyl C–C bond (reaction 85) and abstraction of a benzylic H by OH, H, and O_2:

$$C_6H_5C_2H_5 + X \rightarrow C_6H_5CHCH_3 + XH \rightarrow C_6H_5C_2H_3 + H + XH \quad (101\text{–}103)$$

These reactions are expected to be the primary consumption paths for ethylbenzene.[44] Because the intermediate $C_6H_5CHCH_3$ is expected to decompose solely to styrene, $C_6H_5C_2H_3$, it was not included in the separate reactions of Table IV.

Similar to phenoxy,[39] the methylphenoxy formed in reaction 75 reacts further through combination with H atoms

$$OC_6H_4CH_3 + H \rightarrow HOC_6H_4CH_3 \qquad (104)$$

or by decomposition to methylcyclopentadienyl radical, $C_5H_4CH_3$, and CO as described in the *p*-methylanisole, $CH_3C_6H_4OCH_3$, work of Emdee et al.:[45]

$$OC_6H_4CH_3 \rightarrow C_5H_4CH_3 + CO \rightarrow C_6H_6 + H + CO \qquad (105)$$

Since it was determined by Emdee et al.[45] that methylcyclopentadienyl rearranges quickly to benzene and H atom at flow reactor conditions, methylcyclopentadienyl was not included in the model.

Formation of cresol by methyl addition to phenoxy[46] was initially included using the estimated rate constant of Lin and Lin,[37] but this reaction was found to be a negligible producer of cresol and was thus omitted.

(ii) Comparison of the Model and the Experimental Data. The results of the calculations are shown in Figures 7 and 8. The toluene model did very well at predicting the fuel consumption rate as well as the concentrations of many of the aromatic intermediates including benzene, benzaldehyde, ethylbenzene, benzyl alcohol, and styrene for both lean and rich conditions. The concentrations of both phenol and cresol were, however, always underpredicted.

The figures show that the amounts of acetylene suggested by the model are at least a factor of 2 larger than the experimentally measured values. All of the acetylene comes from the C_4 species which, although not shown, were underpredicted by the toluene model. Thus, even though the C_2's and C_4's were predicted with

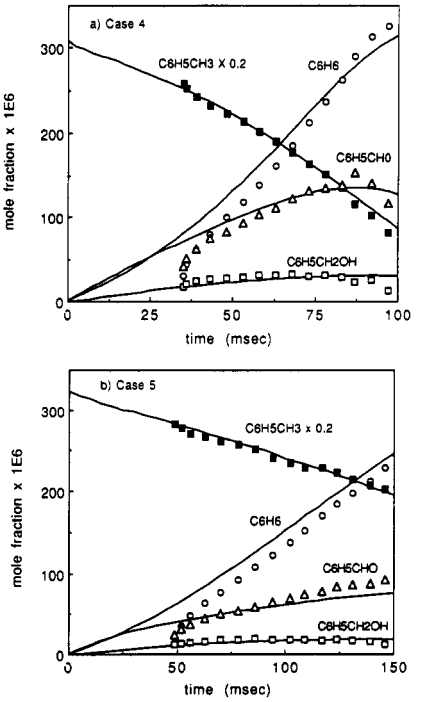

Figure 7. Experimental (symbols) and model predicted (lines) profiles for toluene and several major intermediate species. The experimental data for cases 4 and 5 were shifted in time by +33 and +45 ms, respectively; see text for further discussion.

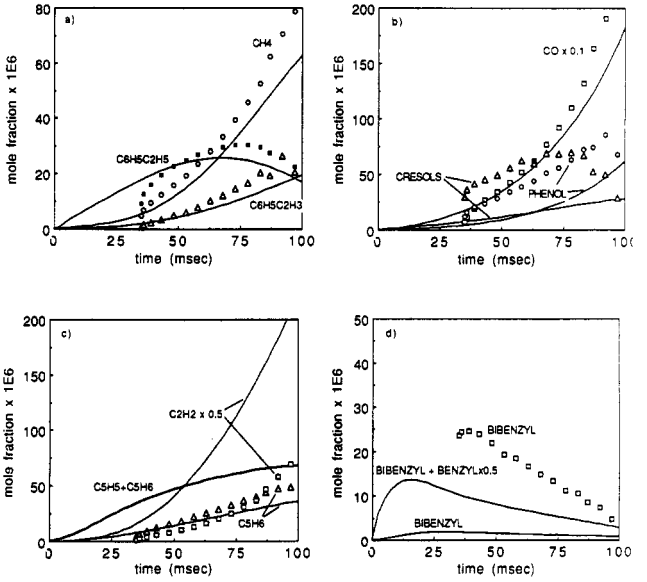

Figure 8. Experimental (symbols) and model predicted (lines) intermediate species profiles for case 4.

fair agreement for the oxidation of benzene near 1100 K, the higher temperature (≈1190 K) oxidation model of toluene suggests that the decomposition rate of the C_4's to the C_2's (e.g., reaction 31) may not have the correct temperature dependence.

In contrast to the benzene oxidation model in which CO was underpredicted, the CO concentrations predicted by the toluene model matched well with the experimental data. The better CO prediction by the toluene model can be partially attributed to the greater understanding of side-chain chemistry which dominates the early oxidation of toluene as compared to the limited understanding of ring chemistry which was important in the oxidation of benzene.

Figure 8d compares the benzyl/bibenzyl model predictions to the bibenzyl profiles from the experimental measurements. Litzinger[7] argued that, due to the weak central C–C bond of bibenzyl, most of the experimentally detected bibenzyl was formed by combination of benzyl in the quench region of the sample probe

(44) Litzinger, T. A.; Brezinsky, K.; Glassman, I. *Combust. Flame* **1986**, *63*, 251.
(45) Emdee, J. L.; Brezinsky, K.; Glassman, I. *J. Phys. Chem.* **1991**, *95*, 1626.
(46) Mulcahy, M. F. R.; Williams, D. J. *Aust. J. Chem.* **1965**, *18*, 20.

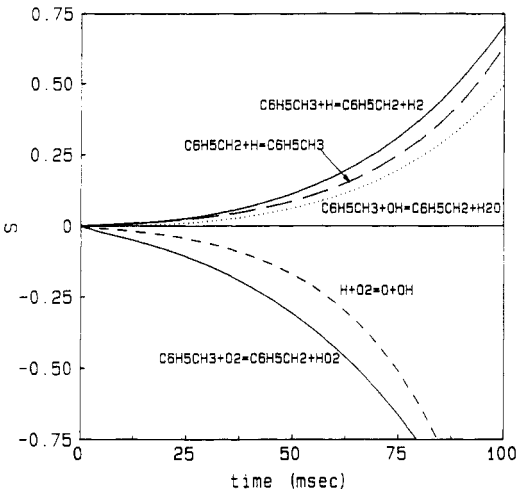

Figure 9. Linear sensitivity coefficients, S, for reactions that affect the toluene species profile for case 4.

rather than in the flow reactor. The model results support those arguments since very little bibenzyl is predicted by the model and the sum of the bibenzyl and one-half of the benzyl mole fractions is comparable to the measured amount of bibenzyl. The fact that the sum is less than the measured bibenzyl mole fraction suggests that the benzyl radical concentration is being underpredicted by the model.

(iii) Reaction Path Analysis. A flux analysis yielded the following information:

1. Reaction 72 is the largest consumer of the fuel followed by reaction 73.

$$C_6H_5CH_3 + OH \rightarrow C_6H_5CH_2 + H_2O \quad (72)$$

$$C_6H_5CH_3 + H \rightarrow C_6H_5CH_2 + H_2 \quad (73)$$

Only about 10% of the fuel reacts through reaction 71.

$$C_6H_5CH_3 + O_2 \rightarrow C_6H_5CH_2 + HO_2 \quad (71)$$

2. The HO_2 and O atom reactions (reactions 80–83) dominate the benzyl consumption.

3. Unlike pyrolysis systems, reaction 69

$$C_6H_5CH_2 + H \rightarrow C_6H_5CH_3 \quad (69)$$

is not at equilibrium but instead proceeds mainly in the recombination direction due to the large concentration of benzyl. Therefore, the ability of benzyl to act as a sink for H atoms is similar to the situation found for both cyclopentadienyl and phenoxy in the benzene submodel.

(iv) Sensitivity Analysis. The results of the sensitivity analysis for toluene are shown in Figure 9. This figure shows that the toluene profile was most sensitive to the following five reactions:

$$H + O_2 \rightarrow O + OH \quad (41)$$

$$C_6H_5CH_2 + H \rightarrow C_6H_5CH_3 \quad (69)$$

$$C_6H_5CH_3 + O_2 \rightarrow C_6H_5CH_2 + HO_2 \quad (71)$$

$$C_6H_5CH_3 + OH \rightarrow C_6H_5CH_2 + H_2O \quad (72)$$

$$C_6H_5CH_3 + H \rightarrow C_6H_5CH_2 + H_2 \quad (73)$$

with the highest sensitivity calculated for reaction 71. The rate constants for all but reaction 71 have been measured experimentally by other investigators.

The inhibitory nature of reaction 69, a termination reaction, is obvious and is indicated by a positive sensitivity coefficient. It is interesting to point out that the sensitivity analysis indicates that reaction 72 and 73 have positive sensitivity coefficients and are thus also inhibitory. This is unusual for reactions which are the primary consumption reactions for the fuel. The reason for this behavior can be traced to the fact that, in both reaction 72 and 73, a very reactive radical (H or OH) is replaced by the unreactive benzyl radical.

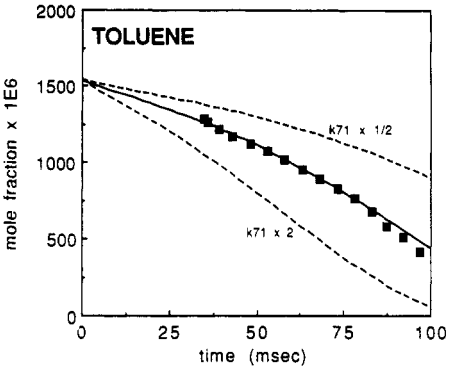

Figure 10. Model predictions (lines) and experimental data (symbols) for case 4 showing the sensitivity of the toluene profile to the rate constant for reaction 71 $C_6H_5CH_3 + O_2 \rightarrow C_6H_5CH_2 + HO_2$.

The high sensitivity of the fuel profile to the rate of reaction 71 is due to the production of HO_2 by that reaction. As stated earlier, the reaction of HO_2 with benzyl is one of the primary consumption steps for benzyl and can lead to the formation of benzaldehyde, H and OH (reaction 82). Because of the high sensitivity of the fuel profile to reaction 71, it was possible to estimate the rate constant parameters for this reaction with reasonable confidence. The activation energy was estimated by the endothermicity of the reaction and the preexponential factor was adjusted to achieve the best fit to the experimental toluene profiles. This method yielded a value of

$$k_{71} = 3 \times 10^{14} \exp(-(41400 \text{ cal/mol})/RT) \text{ cm}^3/\text{mol/s}$$

This value can be compared to a value of $3.3 \times 10^{14} \exp(-(38\,000 \text{ cal/mol})/RT)$ $\text{cm}^3/\text{mol/s}$ fit by Bittker.[10] At 1188 K, Bittker's[10] value is almost 5 times the value used in this study. The effect of changing the rate constant for reaction 71 by a factor of 2 is shown in Figure 10. The high sensitivity suggested by the figure is clear.

In order to test the validity of reactions 80–83, reactions 80 and 81 were replaced by the reactions and branching ratio (BR) suggested by Bartels:[43]

$$C_6H_5CH_2 + O \rightarrow C_6H_5CHO + H \qquad BR = 0.4$$

$$C_6H_5CH_2 + O \rightarrow C_6H_6 + HCO \qquad BR = 0.6$$

Also, for consistency, the products of Bartels et al.[43] were used in reactions 82 and 83 as well. In agreement with the QRRK calculations, the results showed that too little benzaldehyde and too much benzene is produced using Bartels'[43] products.

Finally, the lack of agreement between the cresol profiles should be discussed. The benzene submodel and QRRK calculations discussed earlier indicated that the favored route for O atom addition to the aromatic ring was formation of a phenoxy compound and H atom. In the ≈1100 K benzene model, phenoxy formation was necessary for prediction of the benzene decay rate and furthermore a sufficient amount of phenol was formed through H atom addition to phenoxy. For the ≈1190 K modeling of toluene though, very little phenol/cresol was formed due to the much faster thermal decomposition of phenoxy/cresoxy (reactions 7 and 105) at this higher temperature. Indeed, sensitivity analyses indicated that the cresol profile was sensitive to the rate constant for reaction 105. However, even when the rate constant for reaction 105 was decreased by a factor of 2, the cresol profile was still too low. As was noted previously, the phenoxy decomposition rate determined by Lin and Lin[37] is in need of further experimental study.

IV. Conclusions

By constructing a kinetic model for the oxidation of toluene based on mechanistic and kinetic information from the literature and from thermochemical estimates, it was possible to reasonably model flow reactor oxidation experiments of benzene and toluene. The consumption rate of toluene for both lean and rich oxidation conditions is predicted quite well by the model as are many of

the intermediates including the major species benzaldehyde, ethylbenzene, benzyl alcohol, benzene, and CO. The performance of the model is a significant improvement over previous literature studies.

The inhibitory effect of two major toluene consumption reactions

$$C_6H_5CH_3 + OH \rightarrow C_6H_5CH_2 + H_2O \quad (72)$$

$$C_6H_5CH_3 + H \rightarrow C_6H_5CH_2 + H_2 \quad (73)$$

was clearly indicated by a linear sensitivity analysis. Furthermore, the high sensitivity of the model results to the abstraction reaction

$$C_6H_5CH_3 + O_2 \rightarrow C_6H_5CH_2 + HO_2 \quad (71)$$

allowed for an estimate of this reaction rate constant with reasonable confidence. The results suggest that reaction 71 should be explicitly added to the mechanism in Figure 2 not because it is a primary route for fuel consumption but because it is an important source of HO_2 for the reaction system.

The model showed that the presence of resonantly stable radicals can inhibit the reaction rate by acting as sinks for the H atoms in the system. This behavior was true for both the benzene and toluene models discussed. Thus, the controlling step in the reaction system is not direct oxidation of the fuel but oxidation of the resonant intermediates.

The major shortcomings of the model were found to be the overprediction of acetylene and the underprediction of phenol compounds. The acetylene profiles were not predicted correctly for the higher temperature toluene oxidation even though the lower temperature benzene submodel predicted reasonable levels. With regard to the phenol formation, the temperature dependence of the decomposition rate of phenoxy was expected to be the source of error since phenol was predicted reasonably well in the lower temperature benzene submodel.

This last observation reflects on the use of this model for conditions other than those studied here; because the toluene model has only been verified over a very limited set of concentration, pressure, and temperature conditions, extrapolation beyond these conditions should be considered with great caution. For example, the toluene oxidation model has been combined with the PREMIX code[47] for the calculation of the one-dimensional steady laminar flame speeds of both benzene and toluene flames. The computed values were significantly lower than those reported in the literature, indicating that the chemistry contributing to the flame speed has not been fully captured by the model. An analysis of the sensitivity of the flame speed to the reaction rate coefficients indicates that the calculated flame speeds and the calculated benzene decay profiles for the flow reactor conditions as described in this paper are significantly influenced by the same set of poorly characterized reaction rate coefficients such as those for the decomposition of phenoxy and for its recombination with H atom to form phenol. Consequently, this model should be considered a first step in the development of a more comprehensive model for the high-temperature oxidation of benzene and toluene. As the model is applied to other experimental conditions significant changes in mechanistic steps and in rate coefficients may be necessary to accommodate results covering a wider range of temperatures, pressures, stoichiometries, and concentrations. Nevertheless, the current model successfully predicts the major species profiles measured during the flow reactor oxidation experiments. For those species for which the predictions are not as satisfying, such as for cyclopentadiene, the model very poignantly emphasizes the need for further elementary rate coefficient data and in doing so better defines future directions of research necessary in order to reach the goal of obtaining a truly comprehensive model.

Acknowledgment. The support of this research by the Department of Energy, Office of Basic Energy Sciences, Fundamental Interactions Branch, through Grant DE-FG02.86ER3554 is gratefully acknowledged.

Registry No. $C_6H_5CH_3$, 108-88-3; C_6H_6, 71-43-2.

(47) Kee, R. J.; Grear, J. F.; Smooke, M. D.; Miller, J. A. PREMIX; A Fortran Program for Modeling Steady Laminar One-Dimensional Premixed Flames. Sandia Report SAND 85-8240 UC4, 1985.
(48) TRC Thermodynamic Tables—Hydrocarbons, Thermodynamics Research Center; The Texas A&M University System, College Station, TX (loose-leaf data sheets) extant, 1989.
(49) Burcat, A.; Zelznik, F. J.; McBride, B. J. Ideal Gas Thermodynamic Properties of the Phenyl, Phenoxy, and O-Biphenyl Radicals. NASA Tech. Memo. 83800, 1985.
(50) Weissman, M.; Benson, S. W. *J. Phys. Chem.* **1988**, *92*, 4080.
(51) Ritter, E. R.; Bozzelli, J. W. THERM: Thermodynamic Property Estimation for Radicals and Molecules; computer code, N.J. Institute of Technology, 1987.
(52) TRC Thermodynamic Tables—Non-Hydrocarbons, Thermodynamics Research Center; The Texas A&M University System, College Station, TX (loose-leaf data sheets) extant, 1989.
(53) Ackermann, L.; Hippler, H.; Pagsberg, P.; Reihs, C.; Troe, J. *J. Phys. Chem.* **1990**, *94*, 5247.
(54) Fujii, N.; Asaba, T. *Fourteenth Symposium (International) Combustion [Proceedings]*; The Combustion Institute, Pittsburgh, 1973; p 433.
(55) Madronich, S.; Felder, W. *J. Phys. Chem.* **1985**, *89*, 3556.
(56) Kiefer, J. H.; Mizerka, L. J.; Patel, M. R.; Wei, H.-C. *J. Phys. Chem.* **1985**, *89*, 2013.
(57) Lin, C.-Y.; Lin, M. C. Kinetics of the $C_6H_5 + O_2$ Reaction; Fall Tech. Meeting, East. Sect. Combust. Inst. Paper No. 7, 1987.
(58) Fahr, A.; Stein, S. E. *J. Phys. Chem.* **1988**, *92*, 4951.
(59) Michael, J. V.; Wagner, A. F. *J. Phys. Chem.* **1990**, *94*, 2453.
(60) Miller, J. A.; Mitchell, R. E.; Smooke, M. D.; Kee, R. J. *Symp. (Int.) Combust. [Proc.]* *19* **1983**, 181.
(61) Hippler, H.; Reihs, C.; Troe, J. *Z. Phys. Chem.* **1990**, *167*, 1.
(62) Rao, V. S.; Skinner, G. B. *J. Phys. Chem.* **1989**, *93*, 1864.
(63) Tully, F. P.; Ravishankara, A. R.; Thompson, R. L.; Nicovich, J. M.; Shah, R. H.; Kretter, N. M.; Wine, P. H. *J. Phys. Chem.* **1981**, *85*, 2262.
(64) Robaugh, D.; Tsang, W. *J. Phys. Chem.* **1986**, *90*, 4159.
(65) Kerr, J. A.; Parsonage, M. J. *Evaluated Kinetic Data on Gas Phase Hydrogen Transfer Reactions of Methyl Radicals*; Butterworths: London, 1976.
(66) Muller-Markgraf, W.; Troe, J. *J. Phys. Chem.* **1988**, *92*, 4899.
(67) Robaugh, D. A.; Stein, S. E. *Int. J. Chem. Kinet.* **1981**, *13*, 445.
(68) Solly, R. K.; Benson, S. W. *J. Am. Chem. Soc.* **1971**, *93*, 2127.
(69) Norton, T. S.; Dryer, F. L. *Int. J. Chem. Kinet.* **1990**, *22*, 219.
(70) Norton, T. S.; Dryer, F. L. *Combust. Sci. Technol.* **1989**, *63*, 107.